

NONLINEAR ACOUSTICAL ASSESSMENT OF PRECIPITATE NUCLEATION AND GROWTH IN ALUMINUM ALLOY 2024

John H. Cantrell and William T. Yost
Nondestructive Evaluation Sciences Branch
NASA Langley Research Center
Hampton, VA 23681-2199

INTRODUCTION

The purpose of the present work is to show that measurements of the acoustic nonlinearity parameter in heat treatable alloys as a function of heat treatment time can provide quantitative information about the kinetics of precipitate nucleation and growth in such alloys. Generally, information on the kinetics of phase transformations is obtained from time-sequenced electron microscopical examination and differential scanning microcalorimetry. The present nonlinear acoustical assessment of precipitation kinetics is based on the development of a multiparameter analytical model of the effects on the nonlinearity parameter of precipitate nucleation and growth in the alloy system. A nonlinear curve fit of the model equation to the experimental data is then used to extract the kinetic parameters related to the nucleation and growth of the targeted precipitate. The analytical model and curve fit is applied to the assessment of S' precipitation in aluminum alloy 2024 during artificial aging from the T4 to the T6 temper.

EXPERIMENTS

Samples of stock aluminum alloy 2024-T4 were heat treated in 72 minute increments at a temperature of 190 C for 12 hours according to ASM standards to obtain the transformation from T4 to T6 temper. In order to monitor the changes in the nonlinearity parameter and the hardness during the transformation eleven sets of samples were sectioned in sequence from bar stock. Each set includes two disks, both of nominal radius 15.9 mm and length 6.3mm and 20mm, respectively. Using the first set as the T4 reference, the remaining sets were placed in an oven and heated to (190 ± 5) C. A set was removed every 72 minutes for the 12 hour duration of the heating and quenched in cold running tap water.

The thinner disks of each set (6.3mm thickness) were prepared by polishing the surface and Vickers indentations were made along the diameter of each disk at the center, at a radius of 2.5mm, and at 5 mm. These values were averaged for the hardness value used with each disk. A plot of these values is shown in Fig. 1 (circular data points referred to right ordinate). The error bar shown in the far-right data point represents the typical standard deviation in the measurements.

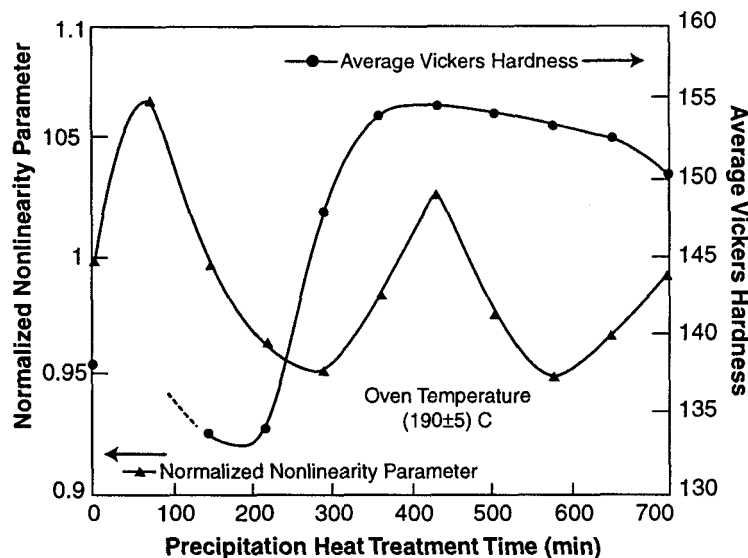


Fig.1. Graph of normalized acoustic nonlinearity parameter (solid triangles) and average Vickers hardness (solid circles) as a function of precipitation heat treatment time of aluminum alloy 2024.

The surfaces of the thicker disks were lapped and polished to a surface parallelism of better than 15 arc seconds and a flatness of better than $0.6\mu\text{m}$. A 12.7 mm diameter lithium niobate (36° Y-cut) compressional wave 5 MHz plate was axially aligned to each sample. Salol (phenyl salicylate) was used to bond the transducer to the sample. The sample-transducer was placed in a capacitive detector apparatus [1], which has an optically flat electrode mounted approximately $7\mu\text{m}$ beneath the sample and axially aligned with the transducer. Acoustic harmonic generation measurements were made on each sample in the manner described by Yost et al. [1,2]. The acoustic nonlinearity parameters were normalized with respect to the value measured for the T4 temper.

The results of these measurements are also given in Fig. 1 which shows a graph of the normalized acoustic nonlinearity parameter (triangular data points referred to left ordinate) plotted as a function of heat treatment time. Although the accuracy of the absolute measurements of the nonlinearity parameter is roughly 5 percent [1,2], the precision of these relative measurements is approximately 1 percent, as indicated by the error bar on the far-left data point.

THEORY

In order to understand the variation in the acoustic nonlinearity parameter as a function of heat treatment time in Fig.1, it is necessary to consider the effects of precipitation on the matrix dislocations. The growth of precipitates causes the matrix dislocations to bow under the action of local precipitate-matrix coherency stresses as illustrated in Fig. 2. Assuming that a given dislocation line roughly follows the contour of

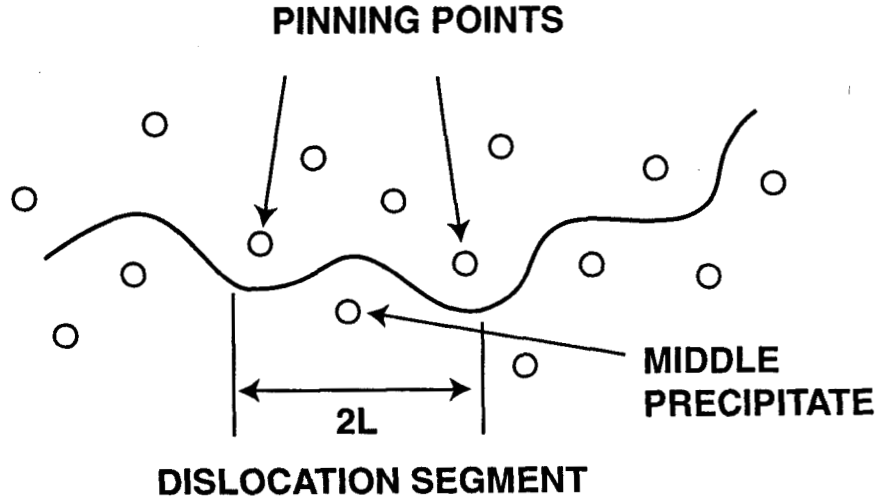


Fig. 2. Bowing (three-point bending) of dislocation segments on a matrix slip plane resulting from local precipitate coherency stresses. The dislocation is represented by the solid curve and the random array of precipitates is represented by circles. The average distance between the pinning points of the bowed dislocation segments is $2L$.

the stress field between adjacent precipitates, Cantrell and Zhang [3] have shown that the stress σ on the dislocation is given by

$$\sigma = -\frac{8G(1+\nu)\delta}{3(1-\nu)} f_p \quad (1)$$

where δ is the precipitate-matrix lattice misfit parameter, G is the shear modulus, ν is Poisson's ratio, and f_p is the volume fraction of precipitate in the material.

It is straightforward to show from the model of Hikata et al. [4] that the fractional change in the acoustic nonlinearity parameter ($\Delta\beta/\beta_0$)

$$\frac{\Delta\beta}{\beta_0} = \frac{24}{5} \frac{\Omega\Lambda^4 R^3 C_{11}^2}{\beta_0 G^3 b^2} |\sigma| \quad (2)$$

where $\Delta\beta$ is the change in the nonlinearity parameter, β_0 is the initial value of the nonlinearity parameter (T4 temper here), L is the dislocation loop length, b is Burgers vector, Λ is the dislocation density, C_{11} is the second order elastic constant, G is the shear modulus, and Ω , R are conversion (Schmid or resolving) factors. Substitution of Eq.(1) into Eq.(2) yields the fractional change in the nonlinearity parameter during precipitate growth as

$$\left(\frac{\Delta\beta}{\beta_0}\right)_{growth} = \frac{64 \Omega \Lambda L^4 R^3 C_{11}^2 (1+\nu) |\delta|}{5 \beta_0 G^2 b^2 (1-\nu)} f_p = a_1 f_p \quad (3)$$

It is important to note here that precipitate growth results in a linear increase in the nonlinearity parameter with increasing volume fraction of precipitate.

Nucleation of a precipitate occurs when a cluster of solute atoms statistically attains a critical radius r_{crit} . Nucleation produces changes in the average dislocation loop length as new precipitates nucleate at sites near dislocations (see Fig. 2). Cantrell and Zhang [3] have shown that the loop length of the dislocation L is related to the critical cluster radius as

$$L = 2 f_p^{-1/3} r_{crit} \quad (4)$$

Substitution of Eq.(4) into Eq.(3) yields the fractional change in the acoustic nonlinearity parameter during nucleation as

$$\left(\frac{\Delta\beta}{\beta_0}\right)_{nucl} = 205 \frac{\Omega \Lambda r_{crit}^4 R^3 C_{11}^2 (1+\nu) |\delta|}{\beta_0 G^2 b^2 (1-\nu)} (f_p^0 + f_p)^{-1/3} = a_2 (f_p^0 + f_p)^{-1/3} \quad (5)$$

where f_p^0 is an effective volume fraction of precipitate resulting from the assumption that, at $f_p = 0$, L has a maximum value

$$L_{max} = 2 (f_p^0)^{-1/3} r_{crit} \quad (6)$$

That is, even in the absence of precipitates dislocations of average length L_{max} behave as if the ends of the dislocations were pinned by precipitates an average distance L_{max} apart, corresponding to a volume fraction f_p^0 . It is important to note from Eq. (5) that precipitate nucleation results in a decrease in the nonlinearity parameter with increasing volume fraction of precipitate.

The kinetics of precipitate nucleation and growth is governed by the Johnson-Mehl-Avrami equation [5]

$$f = 1 - e^{-[k(t-t_0)]^n}, \quad t \geq t_0 \quad (7)$$

where f is the fractional completion of the transformation at a given time t ($f = f_p(t)/f_p^{max}$) and t_0 is the precipitation start time. The kinetic parameter n is a constant (~ 0.5 to 4) governed by the precipitate shape and mode of transformation. The kinetic parameter k is a rate constant that is dependent on both the nucleation and growth rates.

It is assumed that the total fractional change in the nonlinearity parameter ($\Delta\beta/\beta_0$) occurs from the nucleation and growth components as

$$\frac{\Delta\beta}{\beta_0} = \left(\frac{\Delta\beta}{\beta_0}\right)_{growth} + \left(\frac{\Delta\beta}{\beta_0}\right)_{nucl} \quad (8)$$

The Vickers hardness curve in Fig. 1 has a local minimum at roughly 160 min of heat treatment time. Since the value of the Vickers hardness number depends in large measure on the precipitate-matrix coherency stresses, a minimum in the Vickers hardness also

indicates that a minimal volume fraction of strengthening precipitates occurs in aluminum 2024 at 160 min of heat treatment time. For present purposes, it is assumed that the precipitation of S' , the primary strengthening precipitate of AA2024, also begins at this time. For measurements of the nonlinearity parameter starting at time t_0 , it is appropriate to write $f_p = f_p^{\max} f$ and set $t_0 = 160$ min in Eq.(7). Eqs.(3), (5), and (8) then yield the acousto-kinetic expression

$$\frac{\Delta\beta}{\beta_0} \approx a'_2(f^0 + 1 - e^{-[k(t-160)]^n})^{-1/3} + a'_1(1 - e^{-[k(t-160)]^n}) + a_0 \quad (9)$$

where $a'_2 = a_2(f_p^{\max})^{-1/3}$, $a'_1 = a_1 f_p^{\max}$, $f^0 = f_p^0 / f_p^{\max}$, and $a_0 = \text{constant}$. The constant a_0 results from setting the S' precipitation start time at 160 min into the heat treatment time rather than at the time zero, the time to which the experimental data is normalized. The constants a'_1 and a'_2 are calculated from Eqs. (3) and (5) and literature values of the appropriate constants.

CURVE FIT OF ACOUSTO-KINETIC EQUATION AND CONCLUSION

The variation in the acoustic nonlinearity parameter resulting from typical precipitate nucleation and growth mechanisms in metallic alloys is manifested in the acousto-kinetic equation (9) in terms of the kinetic parameters n and k . In general, the values of n and k can be obtained by a nonlinear Levenberg-Marquardt curve fit [6] of the acousto-kinetic equation to appropriate experimental data. The primary strengthening precipitate of aluminum 2024 formed during precipitation heat treatment from the T4 to the T6 temper is the S' precipitate. In order to extract the values of n and k associated with the precipitation of S' , the Levenberg-Marquardt curve fit is applied to that portion of the experimental data specifically involving S' precipitation, but excludes that portion beyond 430 min of heat treatment time. Although S' precipitates continue to grow beyond 430 min (see Fig. 1), a decrease in the acoustic nonlinearity parameter occurs as the result of the loss of precipitate-matrix coherency (overaging). Such loss begins at the peak Vickers hardness (hence, maximum strength) of the material. The coincidence of the S' peak in the nonlinearity parameter curve with the peak of the Vickers hardness curve indicates that measurements of the nonlinearity parameter provide an accurate nondestructive assessment of the optimum aging time (yielding the maximum strength) of the material.

The result of the Levenberg-Marquardt curve fit is shown in Fig. 3, where the normalized acoustic nonlinearity parameter is plotted as a function of heat treatment time over that portion of the total precipitation curve involving S' precipitates. The curve fit yields an n value of 1.43 and a k value of $7.04 \times 10^5 \text{ s}^{-1}$. These values are consistent with that of a diffusion controlled process involving precipitates having a lath structure [5]. The present values of the kinetic parameters are consistent with values obtained on similar alloy systems from independent thermodynamic and electron microscopical assessments [7]. The lath structure of the S' precipitate has been confirmed from electron microscopical examination [8].

An important finding of the present study is that the variation in the acoustic nonlinearity parameter β is manifested as a decrease in β during the nucleation of precipitates, while an increase in β is associated with the growth of precipitates. The experimental data is found to be consistent with these predictions of the analytical model. The distinct effects on the nonlinearity parameter of precipitate nucleation and growth

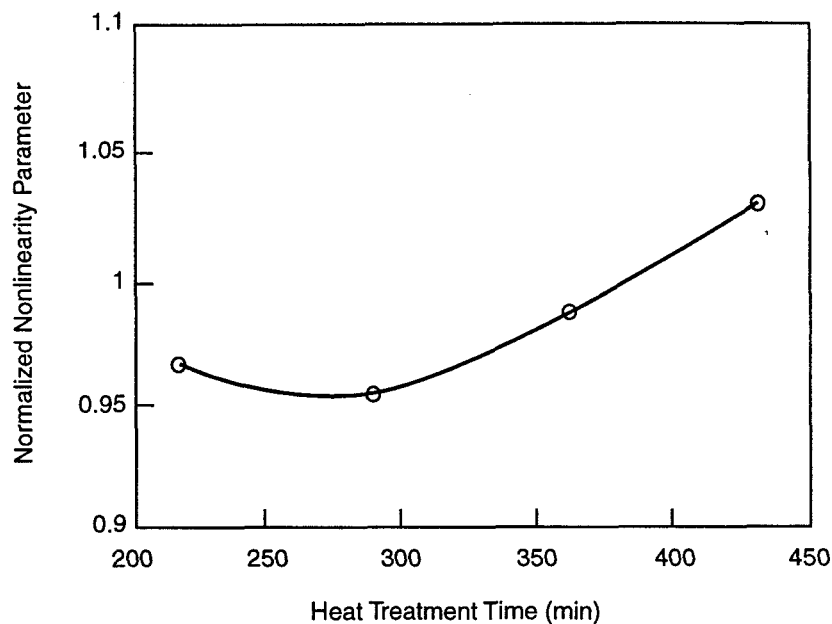


Fig. 3. Nonlinear Levenberg-Marquardt curve fit of the acousto-kinetic equation to the experimental data involving S' precipitates in aluminum alloy 2024.

provide the basis for obtaining the kinetic parameters by curve fitting the acousto-kinetic equation to the experimental data. The agreement between the present results and the thermodynamic-electron microscopical assessment of precipitation in aluminum alloy 2024 indicates that nonlinear acoustical methods may serve as a potentially useful tool complementary to existing methodologies for the characterization of precipitation processes in materials.

ACKNOWLEDGMENTS

This work is supported by the Aging Aircraft Airworthiness Program, NASA Langley Research Center, Hampton, VA, and by a Space Act Agreement with Pratt & Whitney, West Palm Beach, FL.

REFERENCES

1. See, for example, W. T. Yost, J. H. Cantrell, and M. A. Breazeale, *J. Appl. Phys.* 52, 126 (1981).
2. W. T. Yost and J. H. Cantrell, *Rev. Sci. Instrum.* 63, 4182 (1992).
3. J. H. Cantrell and X.-G. Zhang, *J. Appl. Phys.* 84, 5469 (1998).
4. A. Hikata, B. B. Chick, and C. Elbaum, *J. Appl. Phys.* 36, 229 (1965).
5. J. Burke, *The Kinetics of Phase Transformations in Metals* (Pergamon, Oxford, 1965).
6. W. H. Press, B. P. Flannery, S. A. Teukolsky, and W. T. Vetterling, *Numerical Recipes: The Art of Scientific Computing* (Cambridge University Press, Cambridge, 1986), p. 523.
7. A. K. Gupta, P. H. Marois, and D. J. Lloyd, in *Materials Science Forum Vols. 217-222*, eds. J. H. Driver, B. Dubost, F. Durand, R. Fougères, P. Guyot, P. Sainfort, and M. Suéry (Transtec Publications, Zurich, 1996), p. 801.
8. R. N. Wilson and P. G. Partridge, *Acta Metall.* 13, 1321 (1965).